Transaction A: Civil Engineering
Vol. 17, No. 6, pp. 457–470

SCIENTIA
IRANICA

Laboratory Investigations on Wave Run-up and Transmission over Breakwaters Covered by Antifer Units

A. Najafi-Jilani[1,*] and M. Monshizadeh[2]

Abstract. *The effect of a placement pattern of antifer units on the wave run-up and transmission was investigated in more than 380 laboratory tests. The main variables in the experiments were as follows: An antifer unit placement pattern, the breakwater front slope angle, the incoming wave height and steepness, and the still water depth. It was concluded that the wave run-up can be reduced by about 25% by changing the placement pattern from regular to irregular. The measured data were also applied to estimate the wave run-up on the antifer-covered breakwaters as a function of the standard run-up on smooth and impermeable slopes. The measured data of the wave transmission are applied to inspect the prediction equations mentioned in literature, and the predicted and measured data were compared and the deviations were discussed. Some modifications were proposed to improve the accuracy of prediction equations of the wave transmission, especially for breakwaters covered by antifer units in regular and irregular placements.*

Keywords: *Antifer units; Wave run-up; Wave transmission; Placement pattern; Laboratory investigation.*

INTRODUCTION

The wave run-up and transmission due to overtopping are land-ocean interactions that are not yet fully understood. The safe and economical design of breakwaters can be mainly affected by the wave run-up values on their front slope. The transmitted wave height due to overtopping is also one of the most important design parameters. Wave run-up and transmission are majorly dependent on the type and placement pattern of armor units that have covered the front slope of breakwater [1]. Antifer units are widely used as a protective armor layer in rubble mound breakwaters. The wave run-up and overtopping on rubble mound breakwaters have been investigated by many researchers [2,3]. Some investigations were mainly focused on the wave run-up on various types of armor unit, such as rock, Cube, antifer, Accropod, and Tetrapod [4,5]. Neural network techniques were also used to present an appropriate prediction method for wave run-up on each armor unit, based on its significant roughness and permeability [6]. Also, Steendam et al. and Bruce et al. proposed empirical methods to estimate the overtopping discharge, based on the real-state rich databases [7,8], which contain a large variety of overtopping data in the entire world. They developed a major program of tests to establish better the influence of armour roughness and permeability on overtopping. Specifically, their tests determined the relative difference in overtopping behavior for various types of armor unit. They specifically determined the relative difference in overtopping behavior for 13 types or configurations of armor by 179 tests. The various configurations were only investigated for cubic arrangement and it was found that the wave run-up cannot be strongly affected by the placement pattern. However, the effect of placement pattern, especially for antifer armors, was clearly indicated by some other researchers who focused on the placement alternatives of antifer units as a commonly used armor of rubble

1. *Department of Civil Engineering, Islamic Azad University, Islamshahr Branch, Islamshahr, P.O. Box 14138-13561, Iran.*
2. *Water Research Institute, Amir Kabir University of Technology, Tehran, P.O. Box 16765-313, Iran.*
*. *Corresponding author E-mail: a.jilani@iiau.ac.ir*

Received 19 May 2010; received in revised form 18 August 2010; accepted 23 October 2010

mound breakwaters [9]. Although general recommendations and prediction equations were proposed for various types of antifer unit in their excellent laboratory and real scale work, the placement of the antifer units as one of the most effective parameters in the land-wave interaction were not considered in detail. Some researchers developed an experimental model to investigate the stability of antifer units in regular and irregular placement patterns [9]. The stability condition of antifer units in various irregular placement patterns was also investigated by Yagci and Kapdasli [10]. The effect of various irregular patterns of antifer placement on the roughness and porosity of breakwater was also investigated and referenced. A new placement pattern was also suggested by them and evaluated for the stability of units. Although the main stress of this work was on the stability of antifers, they inspected the wave run-up qualitatively, and concluded that it can be significantly affected by the antifer placement pattern. Although their observations about the effect of antifer placement on the wave run-up were mainly qualitative, and so cannot be exactly applied in a detailed comparison, their results show the requirements of a detailed investigation on the antifer placement in a wave run-up and overflow study.

The main objective of this work is to investigate the effect of a placement pattern of antifer units on the wave run-up and transmission. 384 laboratory tests have been performed in a wide range of effective parameters for both the regular and irregular placement of antifer units. The measured data are used to evaluate and improve the prediction methods presented in literature, especially for breakwaters covered by various placements of antifer units.

EXPERIMENTAL SET-UP

Experiments were carried out in a 25 m long, 1 m wide and 2.5 m high wave flume, at the hydro-environmental laboratory of the Water Research Institute in Iran. There were transparent windows at the flume wall for observation of the free water surface profile and wave-breakwater interactions. The experimental set-up included a regular wave maker, located at one end of the flume, and the breakwater section at the other end. Totally, six main variables are considered as the main variable parameters in the performed experiments. These variables are as follows: the placement patterns of antifer units including regular and two different irregular patterns, the front slope angle of the breakwater (α) in a range between 1 to 2.5 for $\cot\alpha$, the incident wave height (H_i) in a range between 8 to 20 cm, mean water depth (h_0) as 80 and 120 cm, the incident wave period (T) in a range between 0.8 to 1.5 s, and the truncated height of the breakwater (H_r) as 85 and 125 cm. The truncated breakwater

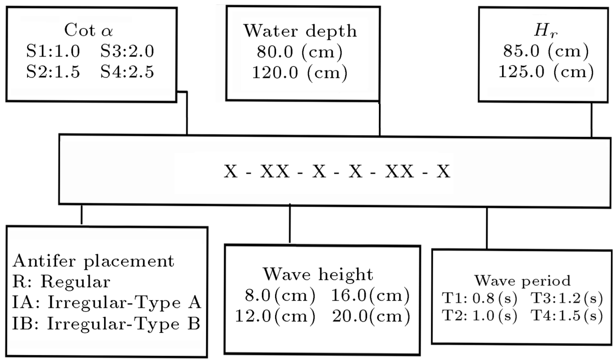

Figure 1. Numbering procedure and definition of main variables in laboratory tests.

was only applied to study the wave transmission due to overtopping. 384 laboratory tests were performed considering the mentioned range of main variables. The exact values of each main variable are depicted in Figure 1, which shows the numbering procedure of the laboratory tests. All specifications of each test can be determined by using its number. The water surface fluctuations were measured at three points located at the central axis of the flume using Validyne DP15 differential pressure transducers (DPD-DP15). The locations of wave gauges, ST1 to ST3, are shown in Figure 2. As illustrated in this figure, the wave characteristics were recorded at two points seaward of the breakwater (ST1 at about 10m from the breakwater and ST2 just before it) and one point at its landward (ST3 only used in wave transmission tests).

The wave reflection analysis is carried out using simultaneous measurements of the waves at several locations along the flume in front of the experimental breakwater [11-13]. In each experimental case, the wave maker input signal was firstly adjusted at the incident wave period and height. But, during a continuously sensing along 100 waves, the effect of reflected waves on the ST2 gauge (exactly in front of the experimental beach) was analyzed. Comparing the recorded data at ST2 and the wanted wave characteristic in each test case, the appropriate correction was made in the input signals of the wave maker. As a result, the recorded wave data at ST2 modified into wanted wave characteristics, which are reported as the incident wave characteristics in each test case. After the analysis, the input signal on the wave maker was not exactly the wanted incident wave period and height, but the recorded wave characteristic at the ST2 gauge, immediately in front of the breakwater, was accurately adjusted to the wanted incident wave characteristics. Based on the detailed analysis in 100 wave numbers in more than 380 tests, the relative error for the incident wave height was about 2% and, for the wave period was about 3.5%, which can be acceptable.

The wave period in the experiment was measured

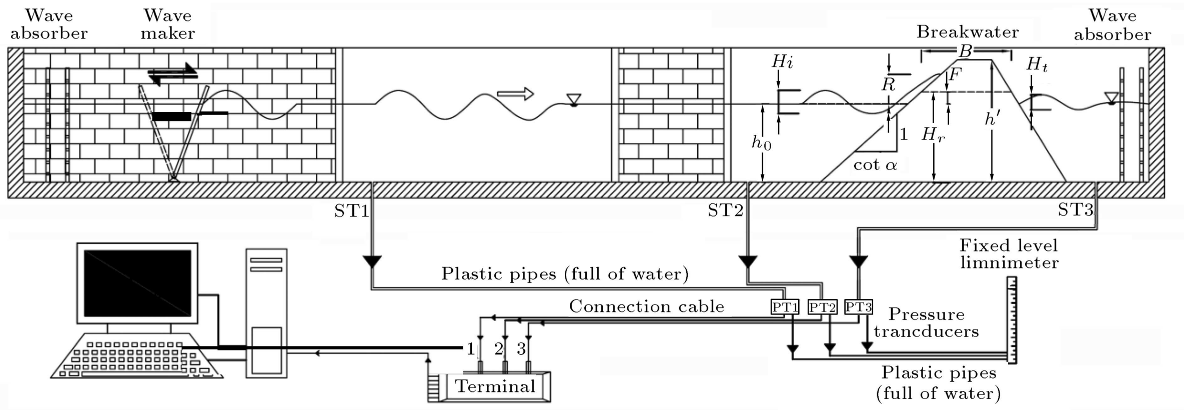

Figure 2. Experimental set-up and definition of main parameters in the laboratory tests.

directly from recorded data at ST1 and ST2 wave gauges. One temporary wave probe at the middle distance between these two gauges was also applied to record the wave time series. The measurements were applied to calculate the water wave celerity at a fixed distance through the flume. Based on the water wave celerity, the wave period and length were calculated.

The wave run-up caused by regular wave trains impinging on various types of smooth and rough sloping structure can be assumed as the basic criterion to investigate the irregular wave run-up on the breakwaters. In other words, the real sea states are simulated by an irregular wave spectrum, but the main concern in this simulation of irregular wave run-up research is to select the most appropriate irregular wave height (H_s, $H_{90\%}$ etc.) and period (T_p, T_z etc.) that can be applied to prediction formulas to estimate the wave run-up in a real sea state. This selection can be made using verified and reliable experimental results and estimation guidance using regular wave flume measurements. Comparing irregular wave flume results with corresponding regular wave flume data, especially for wave run-up and transmission, is a common approach in recent studies.

The main components of the experimental set-up and definition of the main parameters are also shown in Figure 2. Detailed specifications of materials used in various layers of breakwater are listed in Table 1. The location of each layer, including core (layer I), filter layer (layer II-a), under layer (layer II), stone layer (layer III-a) and stone toe (layer III) are illustrated in Figure 3. The stone layer was covered by two armor layers using antifer units, as shown in Figure 3. All specifications of wave gauges are listed in Table 2. Transducers used in experiments have a fast response to changes of pressure. Validyne reluctance sensors, used in this work as wave gauges, have only a single moving part; the sensing diaphragm. The diaphragm is free to move quickly as the pressure changes. There are no links or any other mechanical connections to slow the

Table 1. Specifications of the breakwater layers used in laboratory tests; the location of layers are shown in Figure 4.

Layer	Type	Weight (gr) Upper Limit	Weight (gr) Lower Limit	Volume (m^3)
I	Core	0.44	0.03	4.683
		50% > 0.13		
II-a	Filter	4.39	0.88	0.344
		50% > 2.63		
II	Under layer	487.79	17.56	1.880
		50% > 52.67		
III-a	Stone layer	351.17	175.58	0.111
		50% > 263.4		
III	Stone toe	263.37	87.79	0.334
		50% > 175.6		

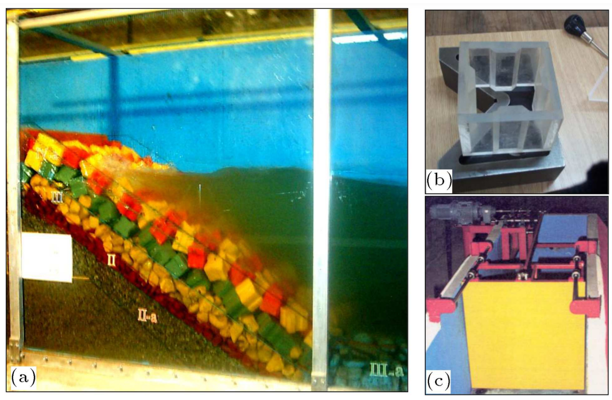

Figure 3. (a)Various layers of breakwater which are covered by two layers of antifer units in laboratory tests. (b) Plexyglass formwork used for antifer construction. (c) Regular wave maker used in experiments.

Table 2. Specifications of wave gauges.

No.	Gauge Station	Sensor Technical Name	$P_{\max}$ (a)	Ac.(b)
1	ST1	DP-15-32- N-1-S-5A	1400	± 3.5
2	ST2	DP-15-22- N-1-S-5A	140	± 0.35
3	ST3	DP-15-22- N-1-S-5A	140	± 0.35

(a): $P_{\max}$: Maximum measurable differential pressure (Δp between two sides of diaphragm) (mm H_2O)

(b): Ac. : Accuracy (mm H_2O)

sensor down. These wave gauges have extremely small displacement volumes. It needs just 6.0E-4 cubic inches (9.8 cubic millimeters) of fluid to go from 0 to full scale reading. The response time of the used wave gauges is 0.0033 (1/300) seconds. The gauges were calibrated before the commencement of the experiments.

A digital camera was used to capture the wave run-up over the breakwater front slope. The camera was fixed perpendicular to the experimental breakwater section. The front transparent wall of the flume at the location of the breakwater section was regionally meshed in one-millimeter steps in each direction. On the front of the breakwater slope, a two scaled ruler was fixed to increase the accuracy of the captured wave run-up on the slope. In each laboratory test case, 100 wave numbers were considered and the maximum wave running up of the water over the breakwater slope was reported as the wave run-up. The preliminary tests were also conducted to find the best location of the camera for more accuracy in capturing the wave run-up. Some test cases (about 25% of all 384 cases) were repeated two or three times to minimize the changes in the measurements and to increase the repeatability and reliability of the measured values of wave run-up.

The placements of the antifer units were considered in three different patterns: regular, irregular-type A, and irregular-type B. These patterns are shown in Figure 4. As shown in this figure, the irregular placement in the A-type is created by rotating the antifer units in the slope plane about 45°. The pattern of irregular placement B-type is made by rotating antifer units around the normal axis of the slope. The regular pattern is equal to the "sloped wall placement pattern", which was indicated in [10]. The specific weight of the antifer units was in the range of 2.2 to 2.4 t/m^3. It was exactly followed by Yagci et al. [9,10]. The concrete compression resistance was between 210-240 kg/cm^2.

Laboratory tests were carried out in two main series. In the first, the wave run-up on the breakwater front slope was measured. In these tests, the total height of breakwater was set as 150 cm without any overflow on the breakwater section. The incident waves were non breaking in all test cases whose wave run-ups were measured. In the second, the height of the breakwater section was truncated to allow wave overtopping, and the transmitted wave height was measured. Detailed investigations on the measured data are discussed in the following sections.

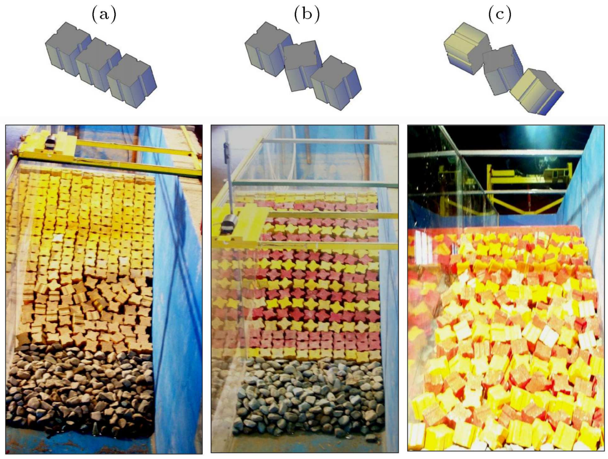

Figure 4. Various placement of the antifer units; (a) regular placement, (b) irregular placement-type A, and (c) irregular placement-type B, used in laboratory tests.

WAVE RUN-UP DATA AND ANALYSIS

The main goal of an investigation into wave run-up is to inspect the effect of the placement pattern of antifer units on the wave run-up. The inspection is made in a wide range of effective parameters and also in various placement patterns of antifer units. A sample of a measured wave run-up is listed in Table 3. Testing conditions in each case can be obtained from its name, using Figure 1. The variation of wave run-up vs. wave height is illustrated in Figure 5, in a dimensionless form. The dashed lines in this figure are passing through the average of the data. As shown in this figure, the effect of the antifer placement pattern on the wave run-up is considerable. The wave run-up has more than a 25% reduction from a regular to irregular pattern (type B) of placement. This effect is relatively the same in various ranges of slope angle, from $\cot\alpha =$ 1 to 2.5. It can be concluded that for steeper slopes, the effect of placement pattern on the wave run-up is increased. At the steepest slope ($\cot\alpha = 1$), the wave run-up for the same incident wave height and steepness is decreased more than 20%, only by changing the placement pattern of antifer units from regular to irregular-type B. The wave run-up is decreased about 10% by changing the placement pattern from regular to irregular-type A. It can be concluded that the wave run-up was affected by more irregularity in this pattern and significantly reduced. This result was qualitatively concluded by Yagci et al. [9,10]. They concluded that

Table 3. Measured data for wave run-up (R) on the breakwater front slope covered by various placements of antifer units; the tests condition in each case can be obtained from its number using Figure 1 (continued).

Case No.	Test No.	R (cm)	Case No.	Test No.	R (cm)	Case No.	Test No.	R (cm)	Case No.	Test No.	R (cm)
1	R-S1-8-80-T1	10.65	97	R-S4-8-80-T1	12.31	193	IA-S3-8-80-T1	9.78	289	IB-S2-8-80-T1	7.46
2	R-S1-12-80-T1	16.63	98	R-S4-12-80-T1	19.23	194	IA-S3-12-80-T1	17.36	290	IB-S2-12-80-T1	11.98
3	R-S1-16-80-T1	22.83	99	R-S4-16-80-T1	26.39	195	IA-S3-16-80-T1	23.25	291	IB-S2-16-80-T1	15.17
4	R-S1-20-80-T1	29.18	100	R-S4-20-80-T1	33.73	196	IA-S3-20-80-T1	27.76	292	IB-S2-20-80-T1	19.22
5	R-S1-8-80-T2	11.01	101	R-S4-8-80-T2	12.73	197	IA-S3-8-80-T2	10.48	293	IB-S2-8-80-T2	8.49
6	R-S1-12-80-T2	17.20	102	R-S4-12-80-T2	19.88	198	IA-S3-12-80-T2	16.26	294	IB-S2-12-80-T2	13.26
7	R-S1-16-80-T2	23.60	103	R-S4-16-80-T2	27.29	199	IA-S3-16-80-T2	21.45	295	IB-S2-16-80-T2	19.51
8	R-S1-20-80-T2	30.17	104	R-S4-20-80-T2	34.88	200	IA-S3-20-80-T2	27.50	296	IB-S2-20-80-T2	22.53
9	R-S1-8-80-T3	11.32	105	R-S4-8-80-T3	13.08	201	IA-S3-8-80-T3	11.04	297	IB-S2-8-80-T3	8.13
10	R-S1-12-80-T3	17.68	106	R-S4-12-80-T3	20.43	202	IA-S3-12-80-T3	15.56	298	IB-S2-12-80-T3	14.40
11	R-S1-16-80-T3	24.26	107	R-S4-16-80-T3	28.04	203	IA-S3-16-80-T3	24.82	299	IB-S2-16-80-T3	17.84
12	R-S1-20-80-T3	31.01	108	R-S4-20-80-T3	35.84	204	IA-S3-20-80-T3	27.85	300	IB-S2-20-80-T3	24.90
13	R-S1-8-80-T4	11.70	109	R-S4-8-80-T4	13.53	205	IA-S3-8-80-T4	11.31	301	IB-S2-8-80-T4	9.13
14	R-S1-12-80-T4	18.28	110	R-S4-12-80-T4	21.13	206	IA-S3-12-80-T4	16.47	302	IB-S2-12-80-T4	14.24
15	R-S1-16-80-T4	25.08	111	R-S4-16-80-T4	29.00	207	IA-S3-16-80-T4	26.07	303	IB-S2-16-80-T4	18.54
16	R-S1-20-80-T4	32.06	112	R-S4-20-80-T4	37.06	208	IA-S3-20-80-T4	29.30	304	IB-S2-20-80-T4	23.96
33	R-S2-8-80-T1	11.28	129	IA-S1-8-80-T1	7.90	225	IA-S4-8-80-T1	10.15	321	IB-S3-8-80-T1	7.47
34	R-S2-12-80-T1	17.63	130	IA-S1-12-80-T1	14.01	226	IA-S4-12-80-T1	15.77	322	IB-S3-12-80-T1	12.90
35	R-S2-16-80-T1	24.19	131	IA-S1-16-80-T1	20.97	227	IA-S4-16-80-T1	22.17	323	IB-S3-16-80-T1	17.16
36	R-S2-20-80-T1	30.92	132	IA-S1-20-80-T1	23.86	228	IA-S4-20-80-T1	28.06	324	IB-S3-20-80-T1	22.95
37	R-S2-8-80-T2	11.67	133	IA-S1-8-80-T2	8.69	229	IA-S4-8-80-T2	11.79	325	IB-S3-8-80-T2	9.41
38	R-S2-12-80-T2	18.23	134	IA-S1-12-80-T2	13.52	230	IA-S4-12-80-T2	16.59	326	IB-S3-12-80-T2	13.69
39	R-S2-16-80-T2	25.01	135	IA-S1-16-80-T2	18.73	231	IA-S4-16-80-T2	23.20	327	IB-S3-16-80-T2	20.80
40	R-S2-20-80-T2	31.97	136	IA-S1-20-80-T2	26.94	232	IA-S4-20-80-T2	32.89	328	IB-S3-20-80-T2	22.85
41	R-S2-8-80-T3	11.99	137	IA-S1-8-80-T3	10.15	233	IA-S4-8-80-T3	12.10	329	IB-S3-8-80-T3	8.88
42	R-S2-12-80-T3	18.73	138	IA-S1-12-80-T3	13.84	234	IA-S4-12-80-T3	16.22	330	IB-S3-12-80-T3	13.45
43	R-S2-16-80-T3	25.70	139	IA-S1-16-80-T3	22.30	235	IA-S4-16-80-T3	25.08	331	IB-S3-16-80-T3	17.88
44	R-S2-20-80-T3	32.85	140	IA-S1-20-80-T3	23.92	236	IA-S4-20-80-T3	30.43	332	IB-S3-20-80-T3	24.04
45	R-S2-8-80-T4	12.40	141	IA-S1-8-80-T4	10.95	237	IA-S4-8-80-T4	12.18	333	IB-S3-8-80-T4	9.48
46	R-S2-12-80-T4	19.37	142	IA-S1-12-80-T4	16.18	238	IA-S4-12-80-T4	16.89	334	IB-S3-12-80-T4	14.84
47	R-S2-16-80-T4	26.58	143	IA-S1-16-80-T4	20.45	239	IA-S4-16-80-T4	27.17	335	IB-S3-16-80-T4	20.65
48	R-S2-20-80-T4	33.97	144	IA-S1-20-80-T4	26.35	240	IA-S4-20-80-T4	31.84	336	IB-S3-20-80-T4	24.59
65	R-S3-8-80-T1	11.83	161	IA-S2-8-80-T1	8.99	257	IB-S1-8-80-T1	6.91	353	IB-S4-8-80-T1	9.82
66	R-S3-12-80-T1	18.48	162	IA-S2-12-80-T1	14.84	258	IB-S1-12-80-T1	11.59	354	IB-S4-12-80-T1	14.32
67	R-S3-16-80-T1	25.36	163	IA-S2-16-80-T1	21.30	259	IB-S1-16-80-T1	16.04	355	IB-S4-16-80-T1	17.83
68	R-S3-20-80-T1	32.42	164	IA-S2-20-80-T1	27.54	260	IB-S1-20-80-T1	20.84	356	IB-S4-20-80-T1	25.63

Table 3. Countinued.

Case No.	Test No.	R (cm)	Case No.	Test No.	R (cm)	Case No.	Test No.	R (cm)	Case No.	Test No.	R (cm)
69	R-S3-8-80-T2	12.24	165	IA-S2-8-80-T2	9.83	261	IB-S1-8-80-T2	7.38	357	IB-S4-8-80-T2	9.11
70	R-S3-12-80-T2	19.11	166	IA-S2-12-80-T2	13.76	262	IB-S1-12-80-T2	11.67	358	IB-S4-12-80-T2	12.71
71	R-S3-16-80-T2	26.23	167	IA-S2-16-80-T2	22.29	263	IB-S1-16-80-T2	16.65	359	IB-S4-16-80-T2	18.09
72	R-S3-20-80-T2	33.52	168	IA-S2-20-80-T2	28.49	264	IB-S1-20-80-T2	21.79	360	IB-S4-20-80-T2	23.72
73	R-S3-8-80-T3	12.57	169	IA-S2-8-80-T3	9.91	265	IB-S1-8-80-T3	7.60	361	IB-S4-8-80-T3	9.72
74	R-S3-12-80-T3	19.64	170	IA-S2-12-80-T3	16.36	266	IB-S1-12-80-T3	11.44	362	IB-S4-12-80-T3	14.47
75	R-S3-16-80-T3	26.95	171	IA-S2-16-80-T3	21.25	267	IB-S1-16-80-T3	17.14	363	IB-S4-16-80-T3	21.19
76	R-S3-20-80-T3	34.45	172	IA-S2-20-80-T3	28.46	268	IB-S1-20-80-T3	20.70	364	IB-S4-20-80-T3	22.38
77	R-S3-8-80-T4	13.00	173	IA-S2-8-80-T4	11.09	269	IB-S1-8-80-T4	7.40	365	IB-S4-8-80-T4	10.00
78	R-S3-12-80-T4	20.31	174	IA-S2-12-80-T4	16.92	270	IB-S1-12-80-T4	14.15	366	IB-S4-12-80-T4	16.13
79	R-S3-16-80-T4	27.87	175	IA-S2-16-80-T4	21.65	271	IB-S1-16-80-T4	17.50	367	IB-S4-16-80-T4	21.67
80	R-S3-20-80-T4	35.63	176	IA-S2-20-80-T4	30.75	272	IB-S1-20-80-T4	21.44	368	IB-S4-20-80-T4	26.98

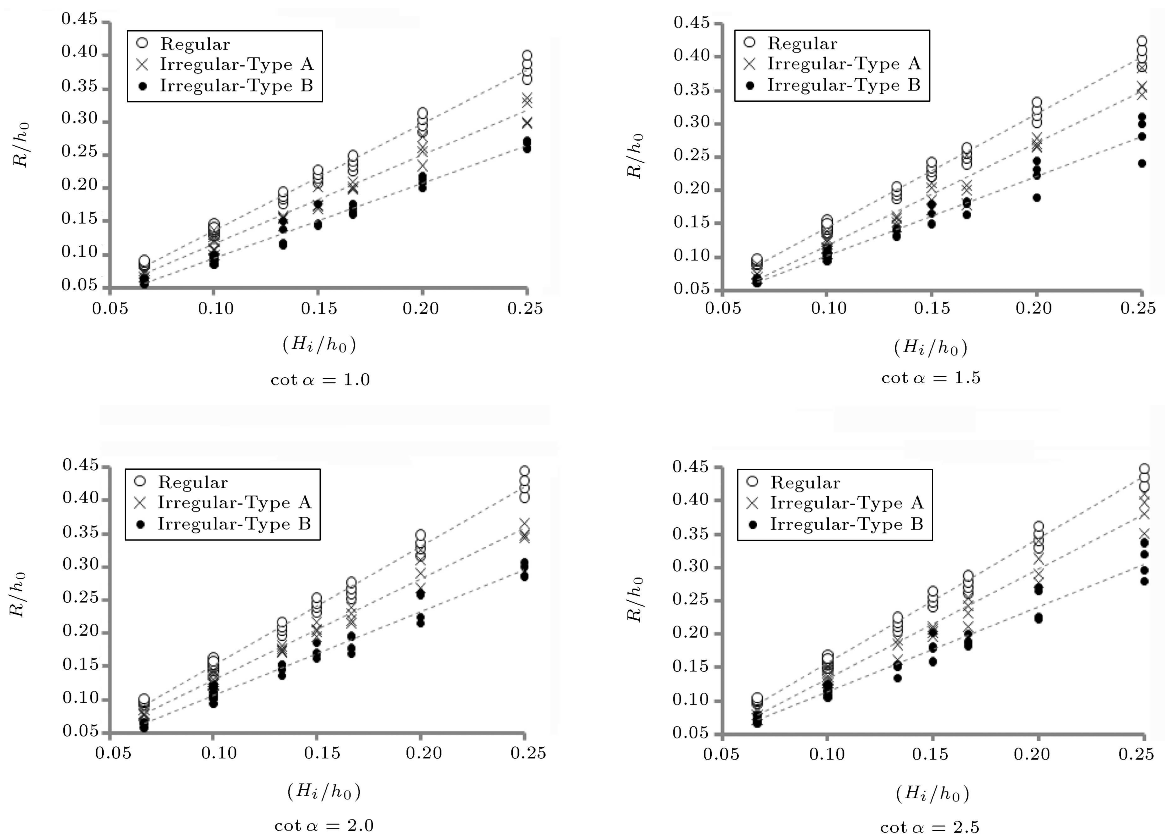

Figure 5. Variation of measured wave run-up (R) vs. incident wave height (H_i) in dimensionless form (divided by still water depth, h_0) over the breakwater covered by antifer units with various placement patterns.

the wave run-up is increased in the regular placement pattern, in our nomination, which they named "sloped wall placement". The increasing of wave run-up was stated as a disadvantage of this pattern, which was caused by low roughness and porosity. antifer units were completely stable in all three placement patterns in the laboratory tests. For a detailed quantitative analysis, the measured data are also used to estimate the wave run-up on the rough and permeable slope of the breakwater. Based on the standard approach for estimation of wave run-up [14], the wave run-up on the rough permeable slopes can be stated as a function of wave run-up in standard case:

$$\left(\frac{R}{h_0}\right)_{\text{rough and permeable}} = f\left(\left(\frac{R}{h_0}\right)_{\text{standard case}}\right), \tag{1}$$

where R is the wave run-up and h_0 is the still water depth. The standard case is the case in which the breakwater slope is smooth and impermeable and the wave is non-breaking. The f function can be empirically determined for each type of armor layer with a specific roughness and permeability. Specifically, for breakwaters covered by two layers of antifer units, Van Der Meer [14] proposed a simple form of f function only multiplying a correction factor, γ_f , to a standard wave run-up. This function is investigated further here by using measured data of wave run-up in the first category of our performed experiments. Research on the estimation of wave run-up in a standard case for non-breaking waves on smooth impermeable slopes has attracted a lot of attention. For instance, Synolakis [15] presented the well-known run-up law in a standard case as:

$$\left(\frac{R}{h_0}\right)_{\text{standard}} = 2.831\left(\frac{H_i}{h_0}\right)^{1.25}.\sqrt{\cot\alpha}. \tag{2}$$

Gedik et al. [16] experimentally examined this empirical equation and obtained good accuracy under standard conditions. Li and Raichlen [17] implied a minor modification in the above equation and came up with:

$$\left(\frac{R}{h_0}\right)_{\text{standard}} = 2.831.(\cot\alpha)^{\frac{1}{2}}\left(\frac{H_i}{h_0}\right)^{\frac{5}{4}} + 0.293.(\cot\alpha)^{\frac{3}{2}}\left(\frac{H_i}{h_0}\right)^{\frac{9}{4}}. \tag{3}$$

Hughes [18] performed some laboratory experiments and introduced the momentum flux of incident wave as an effective parameter for wave run-up under standard conditions. He predicted non-breaking wave run-up over impermeable smooth bed as:

$$\left(\frac{R}{h_0}\right)_{\text{standard}} = 1.82(\cot\alpha)^{\frac{1}{5}}\left(\frac{M_F}{\gamma_w h_0^2}\right), \tag{4}$$

where γ_w is the water density. The dimensionless momentum flux of the incident wave is introduced as:

$$\frac{M_F}{\gamma_w h_0^2} = \frac{1}{2}\left[\left(\frac{H_i}{h_0}\right)^2 + 2\left(\frac{H_i}{h_0}\right)\right] + \frac{N^2}{2M}\left(\frac{H_i}{h_0}+1\right) \left\{\tan\left[\frac{M}{2}\left(\frac{H_i}{h_0}+1\right)\right] + \frac{1}{3}\tan^3\left[\frac{M}{2}\left(\frac{H_i}{h_0}+1\right)\right]\right\}, \tag{5}$$

where M and N are empirical coefficients and can be determined as:

$$M = 0.98\left\{\tanh\left[2.24\left(\frac{H_i}{h_0}\right)\right]\right\}^{0.44}, \tag{6}$$

$$N = 0.69\tanh\left[2.38\left(\frac{H_i}{h_0}\right)\right]. \tag{7}$$

The above mentioned equations were applied to estimate wave run-up under standard conditions of a breakwater front slope (smooth and impermeable). Then, function f, mentioned in Equation 1, was determined in a linear form, as follows, by comparing measured data for antifer-covered breakwater (rough and permeable) with the corresponding standard case:

$$\left(\frac{R}{h_0}\right)_{\text{laboratory measured}} = a\left(\frac{R}{h_0}\right)_{\text{Standard Case}} + b. \tag{8}$$

Based on this comparison, which is illustrated in Figure 6, coefficients a and b in Equation 8 are determined in each placement pattern of antifer units and listed in Table 4. Equation 8 and Table 4 can be used as a guide to estimate the wave run-up on the breakwaters covered by two layers of antifer units in regular and irregular placements using an appropriate formulation for standard wave run-up in literature.

In addition, based on the results of 384 laboratory tests carried out in this work, a new prediction equation is also presented, as follows, to estimate the wave run-up on the slopes covered by antifer units in regular and irregular placement patterns:

$$\frac{R}{h_0} = k_p\left(\frac{\pi}{2\alpha}\right)^{0.18}\left(\frac{H_i}{h_0}\right)^{1.23}\left(\frac{H_i}{L_i}\right)^{-0.15}, \tag{9}$$

where k_p is an empirical coefficient which is related to the placement pattern of antifer units. Based on our performed experiments, the k_p is equal to 1.25, 1.1, and 0.85 for regular and irregular-type A and B, respectively. Equation 9 is developed by minimizing the sum of squared residuals; a residual being the difference between an observed value of wave run-up using laboratory test measurements and the fitted value provided by the formula. The dimensionless groups in Equation 9 are applied based on a dimensional analysis made by Synolakis [15] and revised by Gedik et al. [16]. But the wave steepness is also considered here, which was not included in their prediction approach.

As seen in Equation 9, the appropriateness between wave run-up (R) and incident wave height (H_i) can be derived as

$$R \propto H_i^{(1.23-0.15=1.08)}.$$

So, the direct relation is governed between the incident wave height and wave run-up on the breakwater. It

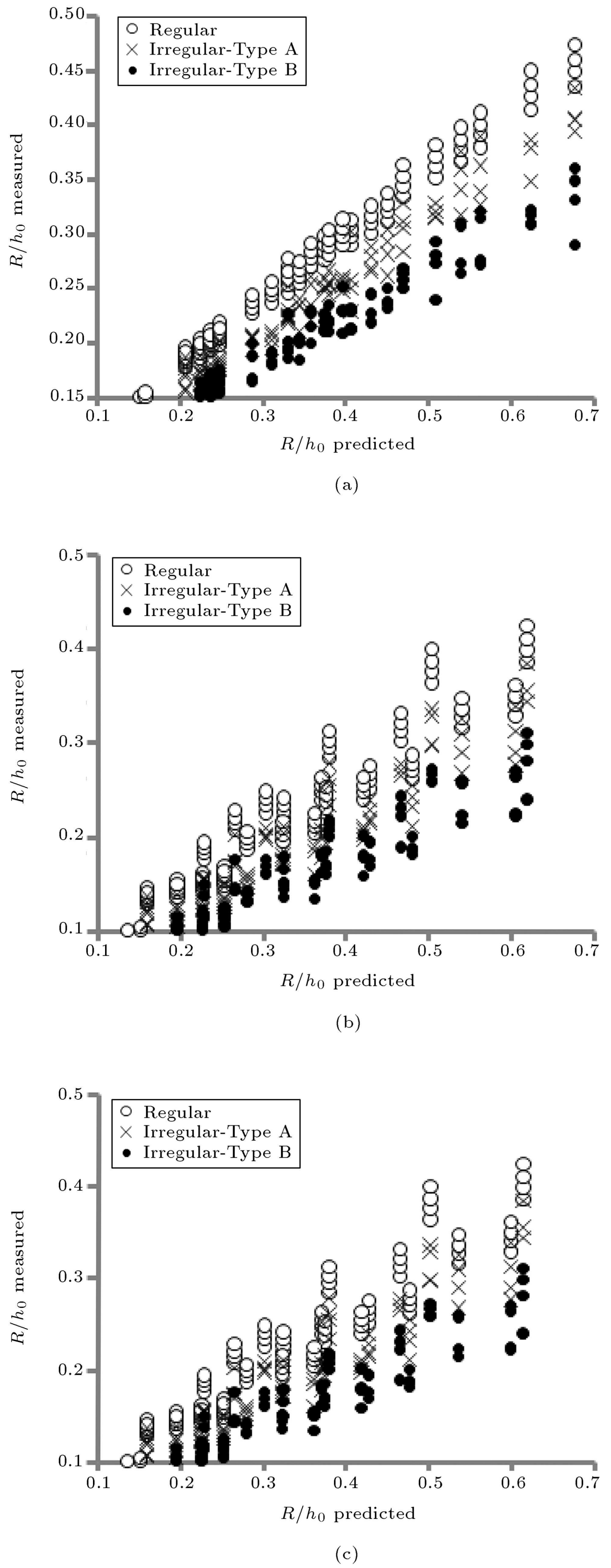

Figure 6. Comparing estimated wave run-up in standard conditions: (a) Hughes [18], (b) Li and Raichlen [17], and (c) Synolakis [15] with the measured data in performed laboratory tests for breakwaters covered by antifer units in various placement pattern.

can be seen that the appropriate boundary condition is considered in the optimization procedure, because the wave run-up goes to zero for zero incident wave height and approches to infinity for infinite wave height. But, the form of the equation is presented in common dimensionless parameters for water waves to be more applicable.

Figure 7 shows the verification of the presented prediction equation using all laboratory measured data for wave run-ups on a breakwater front slope covered by various types of antifer placement. A good agreement can be observed in this figure between predicted values and measured data, and so the reliability of the presented prediction equation, especially for antifer-covered breakwaters, is obtained. The main routes causing more efficiency in the irregular placement pattern of breakwaters are more porosity and roughness in the covered surface of the structure. The irregularity in a three dimensional plane, especially in type B, can cause more water-land involvement and diminish the running up of the wave. This involvement can be increased due to the effect of the package density and surface roughness of armor units. The changes in the velocity domain in both value and direction happen in the irregular placement of antifers related to regular cases.

WAVE TRANSMISSION DATA AND ANALYSIS

In the second category of laboratory tests, the total height of the breakwater was truncated to allow the wave overtopping. As illustrated in Figure 2, h' as the total height of the breakwater was reduced to H_r as truncated height. The maximum transmitted wave height behind the breakwater was measured to determine the wave transmission coefficient. Two main

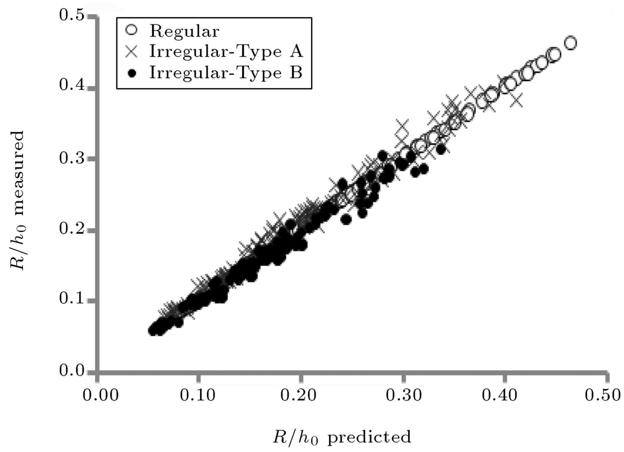

Figure 7. Verification of presented prediction equation of wave run-up on the breakwater front slope covered by two layers of antifer units.

Table 4. Definition of coefficients a and b in Equation 8 to estimate the wave run-up on the breakwaters covered by two layers of antifer units using appropriate standard case (impermeable smooth slope) formulation; the correlation factor (R^2) is also listed.

Wave Run-Up Formula (Standard Case)	**Antifer Units Placement**	a	b	R^2
Hughes [18]	Regular	0.5837	0.0153	0.9897
Hughes [18]	Irregular-type A	0.5071	0.0089	0.9717
Hughes [18]	Irregular-type B	0.4076	0.0115	0.9661
Li and Raichlen [17]	Regular	0.5445	0.0413	0.9367
Li and Raichlen [17]	Irregular-type A	0.4749	0.0309	0.9269
Li and Raichlen [17]	Irregular-type B	0.3812	0.0294	0.9189
Synolakis [15]	Regular	0.5531	0.0395	0.9379
Synolakis [15]	Irregular-type A	0.4824	0.0293	0.9280
Synolakis [15]	Irregular-type B	0.3872	0.0281	0.9202

values were selected for the truncated height of the breakwater (H_r), as 85 cm (for 80 cm water depth cases) and 125 cm (for 120 cm water depth cases). So, the freeboard of the truncated breakwater was fixed at 5 cm. In the truncated breakwater section, the general pattern of layers was the same as illustrated in Figure 3, but the total height of the breakwater decreased to investigate the wave transmission due to overtopping from the breakwater. Totally, in 223 experimental cases, the overtopping condition and meaningful values of the transmitted wave height were measured. The transmitted wave height was measured in overtopping cases exactly behind the breakwater. The measured data were used to determine the ratio of transmitted wave height (H_T) to incident wave height (H_i) in order to calculate the measured wave transmission coefficient ($C_T = H_T/H_i$). A sample (for $\cot\alpha = 1$) of the measured values of transmitted wave height due to overtopping of the breakwater are listed in Table 5. To investigate the wave transmission due to overtopping of the breakwater in all 223 cases, the Seelig formula [19] is considered a pioneer work that is indicated in the Coastal Engineering Manual [20] as:

$$C_T = C\left(1 - \frac{F}{R}\right), \tag{10}$$

where C_T is the wave transmission coefficient due to overtopping ($= H_T/H_i$), F is the freeboard of the truncated breakwater related to the still water level and R is the wave run-up on the breakwater front slope, when the height of breakwater was enough to allow the wave run-up on the slope without any overtopping. These parameters are illustrated in Figure 2. The empirical coefficient, C, was defined as [19,20]:

$$C = 0.5 - \frac{0.11B}{H_r}, \tag{11}$$

where B is the width of the crest of truncated breakwater and H_r is breakwater truncated height. The range of B/H_r in our performed tests is between 0.24 to 1.59, and the range of relative depth ($= h_0/gT^2$ where h_0 is the still water depth and T is the incident wave period) is from 0.04 to 0.19. The predicted values of wave transmission coefficient (C_T) taken from [19,20] are compared with the corresponding measured values, as illustrated in Figure 8. Major differences can be observed between predicted values and laboratory measurements. The average deviation from measured values of the wave transmission coefficient is about 25% in regular or irregular placements of antifer units. Maximum deviation exceeds 150%. The reason may be the differences between the ranges of dimensionless parameters in our experiments and the Seelig pioneer equation. Although the range of B/H_r in our performed tests is included in the range of this

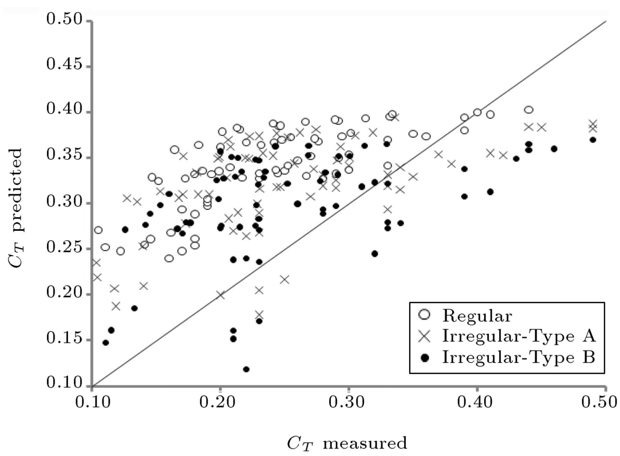

Figure 8. Comparison of wave transmission coefficient between Seelig (indicated in CEM [20]) prediction equation [19] and experimental measurements.

Table 5. Measured data for transmitted wave height (H_T) due to overtopping on the truncated breakwater section; the tests condition in each case can be obtained from its number using Figure 1.

Case No.	Test No.	B (cm)	C_T (Meas.)	Case No.	Test No.	B (cm)	C_T (Meas.)	Case No.	Test No.	B (cm)	C_T (Meas.)
2	R-S1-12-80-T1	70	0.17	130	IA-S1-12-80-T1	70	0.21	258	IB-S1-12-80-T1	70	0.21
3	R-S1-16-80-T1	70	0.23	131	IA-S1-16-80-T1	70	0.28	259	IB-S1-16-80-T1	70	0.28
4	R-S1-20-80-T1	70	0.26	132	IA-S1-20-80-T1	70	0.28	260	IB-S1-20-80-T1	70	0.31
6	R-S1-12-80-T2	70	0.19	134	IA-S1-12-80-T2	70	0.22	262	IB-S1-12-80-T2	70	0.22
7	R-S1-16-80-T2	70	0.27	135	IA-S1-16-80-T2	70	0.27	263	IB-S1-16-80-T2	70	0.28
8	R-S1-20-80-T2	70	0.29	136	IA-S1-20-80-T2	70	0.30	264	IB-S1-20-80-T2	70	0.32
10	R-S1-12-80-T3	70	0.19	138	IA-S1-12-80-T3	70	0.23	266	IB-S1-12-80-T3	70	0.23
11	R-S1-16-80-T3	70	0.23	139	IA-S1-16-80-T3	70	0.29	267	IB-S1-16-80-T3	70	0.29
12	R-S1-20-80-T3	70	0.27	140	IA-S1-20-80-T3	70	0.33	268	IB-S1-20-80-T3	70	0.31
14	R-S1-12-80-T4	70	0.19	142	IA-S1-12-80-T4	70	0.23	270	IB-S1-12-80-T4	70	0.23
15	R-S1-16-80-T4	70	0.25	143	IA-S1-16-80-T4	70	0.29	271	IB-S1-16-80-T4	70	0.26
16	R-S1-20-80-T4	70	0.30	144	IA-S1-20-80-T4	70	0.34	272	IB-S1-20-80-T4	70	0.33
17	R-S1-8-120-T1	30	0.16	145	IA-S1-8-120-T1	30	0.20	273	IB-S1-8-120-T1	30	0.22
18	R-S1-12-120-T1	30	0.28	146	IA-S1-12-120-T1	30	0.33	274	IB-S1-12-120-T1	30	0.32
19	R-S1-16-120-T1	30	0.33	147	IA-S1-16-120-T1	30	0.37	275	IB-S1-16-120-T1	30	0.39
20	R-S1-20-120-T1	30	0.39	148	IA-S1-20-120-T1	30	0.44	276	IB-S1-20-120-T1	30	0.44
21	R-S1-8-120-T2	30	0.17	149	IA-S1-8-120-T2	30	0.23	277	IB-S1-8-120-T2	30	0.21
22	R-S1-12-120-T2	30	0.29	150	IA-S1-12-120-T2	30	0.34	278	IB-S1-12-120-T2	30	0.33
23	R-S1-16-120-T2	30	0.36	151	IA-S1-16-120-T2	30	0.38	279	IB-S1-16-120-T2	30	0.41
24	R-S1-20-120-T2	30	0.41	152	IA-S1-20-120-T2	30	0.45	280	IB-S1-20-120-T2	30	0.44
25	R-S1-8-120-T3	30	0.18	153	IA-S1-8-120-T3	30	0.23	281	IB-S1-8-120-T3	30	0.21
26	R-S1-12-120-T3	30	0.30	154	IA-S1-12-120-T3	30	0.33	282	IB-S1-12-120-T3	30	0.33
27	R-S1-16-120-T3	30	0.35	155	IA-S1-16-120-T3	30	0.42	283	IB-S1-16-120-T3	30	0.39
28	R-S1-20-120-T3	30	0.40	156	IA-S1-20-120-T3	30	0.49	284	IB-S1-20-120-T3	30	0.46
29	R-S1-8-120-T4	30	0.18	157	IA-S1-8-120-T4	30	0.25	285	IB-S1-8-120-T4	30	0.23
30	R-S1-12-120-T4	30	0.33	158	IA-S1-12-120-T4	30	0.35	286	IB-S1-12-120-T4	30	0.34
31	R-S1-16-120-T4	30	0.39	159	IA-S1-16-120-T4	30	0.41	287	IB-S1-16-120-T4	30	0.43
32	R-S1-20-120-T4	30	0.44	160	IA-S1-20-120-T4	30	0.49	288	IB-S1-20-120-T4	30	0.49

parameter in [19] (which was 0 to 3.2), the range of relative depth in [19] the pioneer work (0.003 to 0.06) is majorly different from the range of relative depth in our performed experiments (0.04 to 0.19).

For more investigation, d'Angremond et al. [21] evaluated prediction equations of wave transmission coefficients due to overtopping over the breakwaters:

$$C_T = -0.4\frac{F}{H_i} + 0.64\left(\frac{B}{H_i}\right)^{-0.31}(1 - e^{-0.5\xi}). \qquad (12)$$

ξ is the breaker index (surf similarity parameter or Iribarren Number) as $\xi = \tan\alpha.S^{-0.5}$ where S is the incoming wave steepness ($= H_i/L_i$). This formula is valid for permeable narrow crested breakwaters (where $B/H_i < 8$) and the C_T shall be limited in the lower and upper boundaries as 0.07 and 0.8, respectively. For wide crested breakwaters (where $B/H_i > 8$), the formula was modified as follows by Briganti et al. [22]:

$$C_T = -0.35\frac{F}{H_i} + 0.51\left(\frac{B}{H_i}\right)^{-0.65}(1 - e^{-0.41\xi}). \qquad (13)$$

In our experimental measurements, the ratio of B/H_i was less than 8. So Equation 12 which is presented by

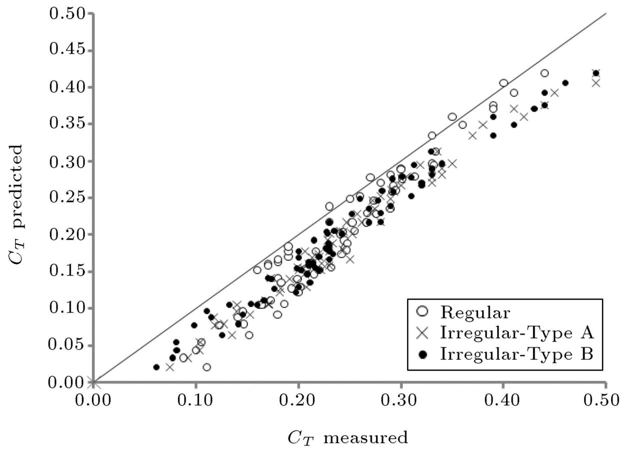

Figure 9. Comparison of wave transmission coefficient between d'Angremond (for $B/H_i < 8$) prediction equations [21] and experimental measurements.

d'Angremond et al. [21] and approved by Briganti et al. [22], is applied. The comparisons of predicted and measured data are illustrated in Figure 9. As shown, the agreement between predicted and measured data is more than the Seelig equation [19]. Also, it seems that some other parameters can influence the wave transmission due to overtopping, and these parameters are not included in the Seelig pioneer work [19]. It can be concluded that the correlation of measured and predicted wave transmission coefficient is affected by the placement pattern of the antifer units. The agreement between predicted and measured data in a regular placement (sloped wall placement in [10]) is relatively more than in irregular cases. In an irregular placement, an average 18% underestimation can be seen in predicted values coming from the equation. The maximum deviation in predicted values is about 28% over laboratory measured data. Based on our performed 223 experimental tests (excluding no-overtopping cases from total number of 384), it can be concluded that the d'Angremond equation [21], which is approved by Briganti et al. [22], can be more applicable and reliable for breakwaters covered by irregular placement of antifer units only by a minor modification. A new prediction equation is presented here only by a minor modification in the d'Angremond equation [21], especially for breakwaters covered by antifer units in regular and irregular placements, which are discussed here (including type A and B presented in Figure 4) as:

$$C_T = -0.45\frac{F}{H_i} + 0.64\left(\frac{B}{H_i}\right)^{-0.25}(1 - e^{-0.6\xi}). \quad (14)$$

For regular placement of an antifer, the modification is not needed and the d'Angremond Equation 12 is validated using our experimental data [21]. This recommendation is valid only for the range of parameters considered in our experimental measurements in wave transmission tests, as follows:

$$0.24 \le \frac{B}{H_r} \le 1.59,$$

$$0.04 \le \frac{h_0}{gT^2} \le 0.19,$$

$$0.25 \le \frac{F}{H_i} \le 0.63,$$

$$1.5 \le \frac{B}{H_i} \le 6.88,$$

$$1.48 \le \xi \le 8.02. \quad (15)$$

The least square method is applied to find the best fit on the observed wave transmission coefficient in various placement patterns of antifers in Equation 14. The dimensionless groups in this formula are the same as used in [21,22]. It was examined again, and it was concluded that the best fit formula can be obtained using the same dimensionless group. But, a modification is made to increase the accuracy and applicability, especially for breakwaters covered by irregular placement patterns on antifer units. A comparison of predicted values, using the new Equation 14, with the measured data in our experimental tests, is illustrated in Figure 10. The maximum deviation of predicted values decreased into less than 3% for wave transmission due to overtopping on the breakwaters covered by the regular or irregular placement of antifer units. The resulted wave transmission coefficient in the above equation is in a range of 0.06 to 0.49, which is relatively included in the recommended range by d'Angremond [21] as 0.07 to 0.8 [21].

A sample water surface displacement time series (η) recorded by each of the three wave gauges is illus-

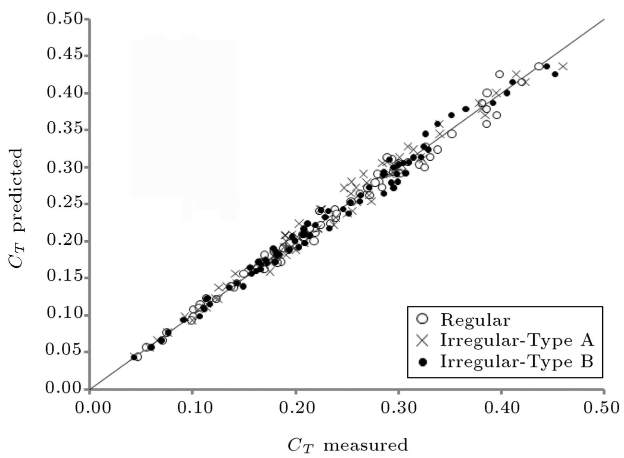

Figure 10. Comparison of wave transmission coefficient between presented prediction equation and experimental measurements.

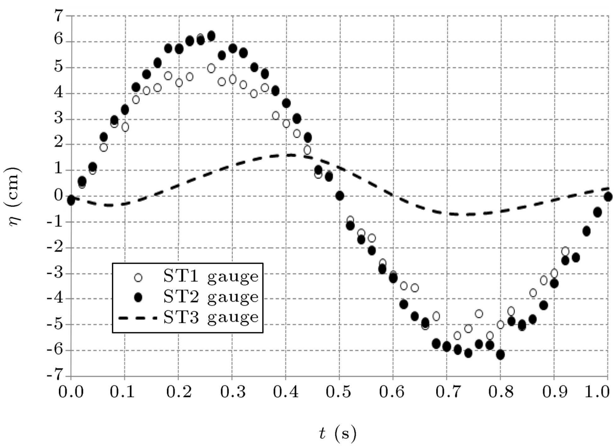

Figure 11. Time series of water surface fluctuation related to still water level at three wave gauges ST1, ST2, and ST3 for test case 6: R-S1-12-80-T2.

trated in Figure 11. In this figure, a sample generated waveform recorded by the first wave gauge closer to the wave generator (ST1) is shown. Theincident waveform recorded by the ST2 wave gauge right in front of the breakwater is also shown in the figure for laboratory test case 6 with test number R-S1-12-80-T2. By adjusting the input data to the wave maker, the wave characteristics near to the paddle (ST1) are tolerated to generate the wanted wave characteristics near to the breakwater (ST2). The transmitted waveform recorded by ST3 right at the lee side of the breakwater is also illustrated in the figure. It shall be considered that the time series are a part of the data under the stable condition of the test, and time $t = 0$ on the graph is not corresponding to the beginning time of the test.

CONCLUSION

More than 380 laboratory tests were carried out to investigate the wave run-up and transmission on breakwaters covered by antifer units. The main variables in the experiments are the antifer unit placement pattern, including regular and two different irregular types, breakwater front slope angle, incident wave height and steepness, still water depth and the truncated height of the breakwater. It was concluded that the effect of antifer placement pattern on the wave run-up is considerable, especially in higher incoming waves. The wave run-up has more than 20% reduction from a regular to irregular pattern of placement. Wave run-up on the antifer-covered breakwaters was stated as a function of the standard condition (i.e. smooth and impermeable slopes). A new run-up prediction equation is also presented and successfully verified. The measured data of wave transmission were applied to investigate the pioneer prediction equation of Seelig [19], which is indicated in [20]. The average difference of predicted and measured values of the wave transmission coefficient in regular or irregular placements of antifer units is about 25%. In addition, the d'Angremond equation [21], which is approved by [22], is also evaluated. It was concluded that in a regular placement of antifers, the agreement between predicted and measured data is relatively more. In irregular placement, an average underestimation of about 18% and a maximum deviation over 28% were observed in all ranges of data. A new prediction equation is presented only by a minor modification in [21]. Less than 3% deviation from measurements was achieved in predicted values of the wave transmission coefficient, especially for breakwaters covered by antifer units in regular and irregular placements.

NOMENCLATURE

α	front slope angle of the breakwater (deg)
γ_w	water density ($MT^{-2}L^{-2}$)
η	water surface fluctuation related to still water level (L)
ξ	breaker index or surf similarity parameter ($-$)
a, b	empirical coefficients in f function ($-$)
B	width of the crest of the truncated breakwater (L)
C	empirical coefficient for estimation of wave transmission (Equation 11) ($-$)
C_T	wave transmission coefficient due to overtopping ($-$)
f	function defined to relate the wave run-up on the antifer-covered slope to wave run-up in standard condition (Equation 1)
F	freeboard of the truncated breakwater related to the still water level ($= h' - H_r$) (L)
g	acceleration due to gravity (LT^{-2})
h_0	still water depth in the laboratory flume (L)
h'	total height of the breakwater section in the experiments (L)
H_i	incoming wave height (L)
H_r	truncated height of the breakwater used in wave transmission tests (L)
H_T	transmitted wave height due to overtopping on the breakwater (L)
k_p	empirical coefficient indicated the placement pattern of antifer units ($-$) in run-up estimation ($-$)

L_i incoming wave length (L)

M, N empirical coefficients to estimate incoming wave momentum flux (Equations 6 and 7)

M_f momentum flux of the incident wave (Equation 5)

S incident wave steepness ($-$)

T incoming wave period (T)

R wave run-up on the breakwater (L)

REFERENCES

1. Hudson, R.Y., Herrmann, F.A., Sager, R.A., Whalin, R.W., Keulegan, G.H., Chatham, C.E. and Hales, L.Z. "Design report on coastal hydraulic models", *USACE Coast. Engrg. Res. Cen.*, **5**, pp. 30-49 (1979).
2. Pozueta, B., Van Gent, M., Van Den Bogaard, H. and Medina, J. "Neural network modeling of wave overtopping at coastal structures", *29th Int. Conf. on Coast. Engrg. (ASCE)*, **3**, pp. 4275-4287 (2004).
3. Van Der Meer, J., Van Gent, M., Pozueta, B., Verhaeghe, H., Steendam, G. and Medina, J. "Applications of a neural network to predict wave overtopping at coastal structures", *5th Int. Conf. on Coast., Struc., and Breakwat.*, **2**, London, UK, pp. 259-268 (2005).
4. Gunbak, A.R. "Antifer cubes on rubble mound breakwaters", *5th Int. Conf. on Coast. and Port Engrg. in Devel. Count. (COPEDEC)*, **3**, Cape Town, South Africa, pp. 135-141 (1999).
5. Gunbak, A.R. "Use of rock, tetrapod, antifer, accropode, core-lock armor units on the rubble mound breakwaters", *6th Int. Cong. of Permanent International Association of Navigation Congresses (PIANC)*, **2**, Buenos Aires, Argentina, pp. 101-107 (2000).
6. Bakhtyar, R., Yeganeh Bakhtiary, A. and Ghaheri, A. "Application of neuro-fuzzy approach in prediction of run-up in swash zone", *J. of Appl. Oc. Res.*, **30**(1), pp. 17-27 (2008).
7. Steendam, G.J., Van Der Meer, J., Verhaeghe, H., Besley, P., Franco, L. and Van Gent, M. "The international database on wave overtopping", *29th Int. Conf. on Coast. Engrg. (ASCE)*, **6**, Lisbon, Portugal, pp. 4301-4313 (2004).
8. Bruce, T., Van Der Meer, J., Franco, L., and Pearson, J.M. "Overtopping performance of different armor units for rubble mound breakwaters", *J. of Coast. Engrg.*, **56**(2), pp. 166-179 (2009).
9. Yagci, O. and Kapdasli, S. "Alternative placement technique for Antifer blocks used on breakwaters", *J. of Oc. Engrg.*, **30**, pp. 1433-1451 (2003).
10. Yagci, O., Kapdasli, S. and Cigizoglu, H.K. "The stability of the Antifer units used on breakwaters in case of irregular placement", *J. of Oc. Engrg.*, **31**(8-9), pp. 1111-1127 (2004).
11. Goda, Y. and Suzuki, Y. "Estimation of incident and reflected waves in random wave experiments", *15th Int. Conf. on Coast. Engrg. (ASCE)*, **4**, Reston, Virginia, USA, pp. 828-845 (1976).
12. Park, W.S., Oh, Y.M. and Chun, I.S. "Separation technique of incident and reflected waves using least squares method", *J. of Korean Soc. of Coast. and Oc. Engrg.*, **4**, pp. 139-145 (1992).
13. Ketabdari, M.J. and Ranginkaman, A. "A simulation of random irregular waves for numerical and physical models using digital filters", *Scientia Iranica, Trans. B: Civil Eng.*, **16**(3), pp. 240-247 (2009).
14. Van Der Meer, J. "Wave run-up and wave overtopping at dikes", *Rep. of Tech. Adv. Comm. on Wat. Def. in Netherland*, **2**, pp. 198-223 (2002).
15. Synolakis, C.E. "The run-up of solitary waves", *J. of Flu. Mech.*, **185**, pp. 523-545 (1987).
16. Gedik, N., Irtem, E. and Kabdasli, S. "Laboratory investigation on tsunami run-up", *J. of Oc. Engrg.*, **32**, pp. 513-528 (2005).
17. Li, Y. and Raichlen, F. "Solitary wave run-up on plane slopes", *Int. J. of Wat., Port, Coast. and Oc. Engrg., ASCE*, **127**(1), pp. 33-44 (2001).
18. Hughes, S.A. "Estimation of wave run-up on smooth, impermeable slopes using the wave momentum flux parameter", *J. of Coast. Engrg*, **118**, pp. 1085-1104 (2004).
19. Seelig, W.N. "Two-dimensional tests of wave transmission and reflection characteristics of laboratory breakwaters", *Tech. Rep.*, **80**(1), U.S. Army Eng. Water. Exper. Sta., 2, Vicksburg, Mississippi, USA, pp. 411-420 (1980).
20. USACE "Coastal Hydrodynamics", *Coastal Engineering Manual (CEM)*, Part II, EM 1110-2-1100, pp. 50-155 (2002).
21. d'Angremond, K., Van Der Meer, J. and De Jong, R.J. "Wave transmission at low crested structures", *25th Int. Conf. on Coast. Engrg, ASCE*, **3**, Florida, USA, pp. 3305-3318 (1996).
22. Briganti, R., Van Der Meer, J., Buccino M. and Calabrese, M. "Wave transmission behind low crested structures", *Int. Conf. on Coast. Struc.*, **2**, Portland, Oregon, USA, pp. 494-503 (2003).

BIOGRAPHIES

Ataollah Najafi Jilani is Assistant Professor of Civil Engineering in the Islamic Azad University, Islamshahr Branch. He earned his B.S. in Civil Engineering in 1995 from Tehran Polytechnic (Amir Kabir) University of Technology, his M.S. in Hydraulic Structures Engineering in 1997 from Tehran University, and his Ph.D. in Civil-Hydraulic Engineering in 2007 from Sharif University of Technology. His major awards were the 22nd Khawrizmi international award (2009) for third rank in applicable research in Iran entitled

"Landslide Generated Waves in Dam Reservoirs". He was the first co-author of this project. He was also in the first rank of graduated Ph.D. students in the Civil Engineering Department at Sharif University of Technology and so earned the Tavakkoli Prize of the Civil Engineering Faculty (2009). He was also in the first rank of graduated M.S. students and earned the graduation ceremony award at Tehran University (1997). Dr. Najafi-Jilani has written 9 journal papers and more than 26 national and international conference papers. The main topics of his research interests are: Numerical and Experimental Investigations on Hydraulic Engineering, Coastal Hydrodynamics, Marine Structures and Coastal Sedimentation.

Morteza Monshizadeh is senior researcher in the Water Research Institute affiliated to the Ministry of Energy, Iran. He earned his B.S. in Mechanical Engineering in 1991 from K.N.T University of Technology and his M.S. in Energy Engineering in 1995 from the Branch of Science and Research of the Islamic Azad University. He is a Ph.D. student in Civil Engineering in Amir Kabir University of Technology. He was selected in the first rank of researchers in the Ministry of Energy in 2001. Mr. Monshizadeh has written 6 journal papers and more than 15 conference papers. His main research interests are: Coastal Engineering, Coastal Sedimentation, Dam Reservoir Sedimentation, and Marine Structures.